Journal of Biomechanics 74 (2018) 106–115

Contents lists available at ScienceDirect

Journal of Biomechanics

journal homepage: www.elsevier.com/locate/jbiomech
www.JBiomech.com

Dynamic balance during walking adaptability tasks in individuals post-stroke

Arian Vistamehr [a], Chitralakshmi K. Balasubramanian [b], David J. Clark [c,d], Richard R. Neptune [e], Emily J. Fox [a,f,*]

[a] Motion Analysis Center, Brooks Rehabilitation, Jacksonville, FL, USA
[b] Department of Clinical and Applied Movement Sciences, University of North Florida, Jacksonville, FL, USA
[c] Brain Rehabilitation Research Center, Malcom Randall VA Medical Center, Gainesville, FL, USA
[d] Department of Aging and Geriatric Research, University of Florida, Gainesville, FL, USA
[e] Department of Mechanical Engineering, The University of Texas at Austin, Austin, TX, USA
[f] Department of Physical Therapy, University of Florida, Gainesville, FL, USA

ARTICLE INFO

Article history:
Accepted 14 April 2018

Keywords:
Community ambulation
Angular momentum
Stability
Obstacle
Biomechanics
Gait

ABSTRACT

Maintaining dynamic balance during community ambulation is a major challenge post-stroke. Community ambulation requires performance of steady-state level walking as well as tasks that require walking adaptability. Prior studies on balance control post-stroke have mainly focused on steady-state walking, but walking adaptability tasks have received little attention. The purpose of this study was to quantify and compare dynamic balance requirements during common walking adaptability tasks post-stroke and in healthy adults and identify differences in underlying mechanisms used for maintaining dynamic balance. Kinematic data were collected from fifteen individuals with post-stroke hemiparesis during steady-state forward and backward walking, obstacle negotiation, and step-up tasks. In addition, data from ten healthy adults provided the basis for comparison. Dynamic balance was quantified using the peak-to-peak range of whole-body angular-momentum in each anatomical plane during the paretic, nonparetic and healthy control single-leg-stance phase of the gait cycle. To understand differences in some of the key underlying mechanisms for maintaining dynamic balance, foot placement and plantarflexor muscle activation were examined. Individuals post-stroke had significant dynamic balance deficits in the frontal plane across most tasks, particularly during the paretic single-leg-stance. Frontal plane balance deficits were associated with wider paretic foot placement, elevated body center-of-mass, and lower soleus activity. Further, the obstacle negotiation task imposed a higher balance requirement, particularly during the trailing leg single-stance. Thus, improving paretic foot placement and ankle plantarflexor activity, particularly during obstacle negotiation, may be important rehabilitation targets to enhance dynamic balance during post-stroke community ambulation.

© 2018 Elsevier Ltd. All rights reserved.

1. Introduction

Community ambulation is a major challenge post-stroke, with only 7% of those discharged from the hospital reporting the ability to walk independently in the community (e.g., Hill et al., 1997). Further, 73% of the community ambulators have been reported to fall within 6 months of discharge from the hospital, with most falls occurring during walking (Forster and Young, 1995). Thus, it is essential to design effective interventions to improve dynamic balance during post-stroke community ambulation. A crucial step in designing effective interventions is to understand and quantify dynamic balance during walking tasks essential to community ambulation.

Walking at home and in the community involves both steady-state walking on level terrains as well as tasks that require walking adaptability such as negotiating obstacles, stepping up on surfaces (e.g., curbs) and walking on uneven terrains. Walking adaptability is the ability to modify steady-state walking pattern to meet task goals and environmental demands (Balasubramanian et al., 2014). Although most studies of post-stroke walking function and dynamic balance have focused on steady-state walking (e.g., Allen et al., 2014; Hall et al., 2012; Nott et al., 2014), walking

* Corresponding author at: Department of Physical Therapy, University of Florida, Box 100154, UFHSC, Gainesville, FL 32610-0154, USA.
E-mail address: ejfox@phhp.ufl.edu (E.J. Fox).

https://doi.org/10.1016/j.jbiomech.2018.04.029
0021-9290/© 2018 Elsevier Ltd. All rights reserved.

adaptability tasks have received little attention (Balasubramanian et al., 2014).

Analysis of whole-body angular-momentum (H) has provided an objective method for assessing dynamic balance in individuals post-stroke during steady-state walking (Nott et al., 2014; Vistamehr et al., 2016). This approach has also been used to quantify dynamic balance in adults with lower limb amputations during steady-state walking (Silverman and Neptune, 2011) and various adaptability tasks (e.g., Pickle et al., 2014; Sheehan et al., 2015), in older adults recovering from a trip (Pijnappels et al., 2005b), and in healthy younger adults (Herr and Popovic, 2008; Neptune and McGowan, 2011, 2016; Silverman et al., 2014, 2012; Yeates et al., 2016).

While the generation of H is essential to walking performance, H is highly regulated in order to maintain dynamic balance (Herr and Popovic, 2008). The regulation of H involves complex multi-level interactions between the central-nervous-system, the neuromechanics of muscle force generation and foot placement, and the resulting net external moment about the body center-of-mass (e.g., Neptune and McGowan, 2016; Pijnappels et al., 2005a, b; Robert et al., 2009). The net external moment, a function of foot placement and ground-reaction-forces (Fig. 1), is equal to the time rate of change of H. Thus, any adaptations in foot placement and generation of ground-reaction-forces can influence the rate of change of H and resulting peak-to-peak range of H (H_R) (e.g., Silverman and Neptune, 2011). Further, simulation studies of healthy adults during walking have shown that the ankle plantarflexors (soleus and gastrocnemius) are primary contributors to the ground-reaction-forces and the key regulators of H in both sagittal and frontal planes (Neptune and McGowan, 2011, 2016). However, it is not clear how foot placement and muscle activation adaptations post-stroke influence the regulation of H and the resulting H_R.

A higher H_R imposes higher balance control demands, which if not met properly during a perturbed condition, can lead to falls (Pijnappels et al., 2005a). Although certain tasks such as stair climbing may demand higher H_R generation than level walking (Silverman et al., 2014), a higher H_R can also result from poor H regulation in those with mobility impairments, suggesting presence of balance deficits. Prior studies of individuals post-stroke have shown that during steady-state walking, those with higher H_R in the frontal plane have poorer Berg Balance Scale (BBS) and Dynamic Gait Index (DGI) scores (Nott et al., 2014; Vistamehr et al., 2016). Further, those classified as fallers based on BBS and DGI scores, poorly regulated their H particularly during the paretic single-leg-stance (SLS), identifying this phase of the gait cycle as a period of higher instability (Nott et al., 2014). The assessment of dynamic balance through the analysis of H in individuals post-stroke has been limited to the frontal plane steady-state level walking. Thus, there are gaps in understanding the regulation of H in other anatomical planes and during tasks requiring adaptability.

The primary purpose of this study was to assess dynamic balance using three-dimensional H in individuals post-stroke and healthy adults across selected walking adaptability tasks and to identify the underlying mechanisms associated with the regulation of H. Our first hypothesis was that across all tasks, significant balance deficits would be evident during the paretic-SLS compared to the nonparetic- and healthy control-SLS. In our second hypothesis, we were most interested in anatomical planes (Fig. 1) where the largest differences in H were present between groups. We hypothesized that individuals post-stroke used different mechanisms for

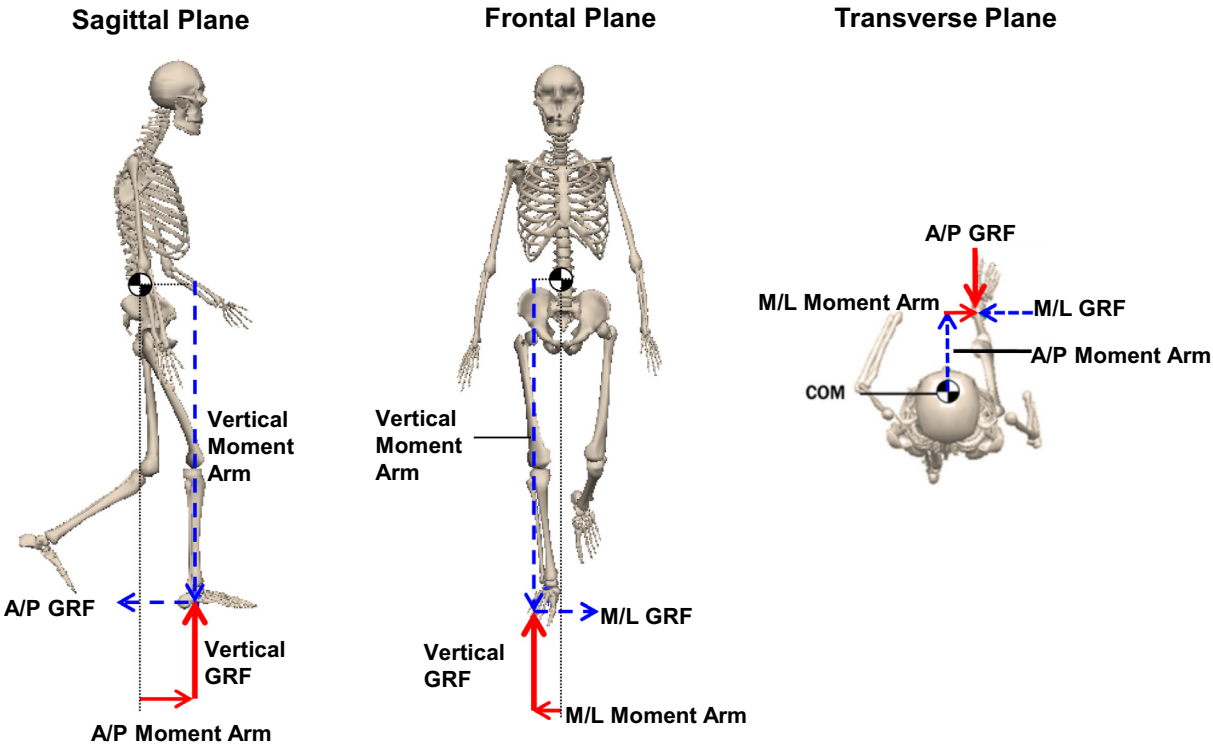

Fig. 1. The net external moment components are shown in the sagittal, frontal and transverse planes during single-leg-stance. Whole-body center-of-mass (CoM) is shown with '●'. The ground-reaction-force (GRF) vectors and their corresponding moment arms appear in the same color. During single-leg-stance, only the stance leg contributes to the net external moment about the body CoM. In each plane, the net external moment consists of two moment arm and GRF components. For instance, in the frontal plane, only the vertical and mediolateral moment arms and GRFs contribute to the net external moment and the regulation of whole-body angular-momentum. Here, we focus on analyzing the moment arms to further understand the regulation of whole-body angular-momentum. (For interpretation of the references to colour in this figure legend, the reader is referred to the web version of this article.)

regulating H than healthy controls as evidenced by their altered net external moment, foot placement, and ankle plantarflexor muscle activity. These results will contribute to our understanding of dynamic balance post-stroke during walking adaptability tasks and may help guide the development of targeted interventions to address deficits in dynamic balance.

2. Methods

2.1. Participants

Fifteen individuals with post-stroke hemiparesis were enrolled (Table 1). The inclusion criteria were: a single stroke primarily affecting unilateral motor function, 18 years or older, able to walk at least 10 m independently or with supervision using a cane or an orthotic device, able to follow verbal requests and no secondary neurological conditions. Participants did not use orthotic or assistive devices during data collection. In addition, data from 10 healthy individuals were collected for comparison (Table 1). The study protocol was approved by the Institutional Review Boards of the collaborating universities and all participants provided informed consent.

2.2. Experimental data collection

A modified Helen Hayes full-body marker set was used to define 15 body segments (head, trunk, pelvis, and each upper arm, lower arm, hand, thigh, shank, and foot). Three-dimensional kinematics were collected at 100 Hz using a 12-camera motion capture system (VICON, Los Angeles, USA) and bilateral surface electromyographic (EMG) data from soleus and medial-gastrocnemius muscles were collected at 2000 Hz using a Trigno™ wireless system (Delsys, Inc., Boston, USA). The tasks included walking forward at self-selected and fastest-comfortable speeds, walking backward at self-selected speed, obstacle negotiation, and step-up tasks. The obstacle negotiation and step-up tasks were divided into trailing and leading phases (Fig. 2). The obstacle dimensions were 20 cm (height), 46 cm (length) and 7 cm (width) and the step-up box was 20 cm (height). For each movement task 3 trials were collected and during each trial participants walked on a 10-meter over-ground walkway. During the obstacle negotiation and step-up tasks, the obstacle and step-up box were placed in the middle of the walkway, respectively. Prior to gait initiation, the participant was instructed to lead with their preferred leg for 3 trials and then lead with the contralateral leg for 3 trials. Participants walked to the obstacle, cleared the obstacle and continued walking to the end of the walkway. Similarly, participants walked to the box, stepped up with both feet, then stepped down and continued walking.

2.3. Data processing

The kinematic data were low-pass filtered using a fourth-order Butterworth filter with cutoff frequency of 7 Hz. A 15-segment model (C-Motion, Inc., Germantown, USA) was used to calculate body center-of-mass (CoM) position and velocity as well as angular-momentum for each segment.

At each numerical time step over the gait cycle, whole-body angular-momentum (H) about the CoM was calculated as:

$$\vec{H} = \sum_{i=1}^{n} \left[(\vec{r}_i^{COM} - \vec{r}_{body}^{COM}) \times m_i (\vec{v}_i^{COM} - \vec{v}_{body}^{COM}) + I_i \overrightarrow{\omega_i} \right] \quad (1)$$

where $\vec{r}_i^{COM}$ and $\vec{v}_i^{COM}$ are the position and velocity vectors of the i-th segment's CoM, respectively. $\vec{r}_{body}^{COM}$ and $\vec{v}_{body}^{COM}$ are the position and

Table 1
Participant characteristics: age, gender, affected side, time since stroke, mass, height, and overground self-selected (SS) walking speed. Walking speed was calculated using the body center-of-mass velocity from the kinematics data.

	Age (years)	Gender	Affected side	Time since stroke (months)	Mass (kg)	Height (m)	SS speed (m/s)
Post-stroke							
1	55	M	R	18	130	1.83	0.81
2	60	F	L	7	88	1.66	0.87
3	64	F	L	12	73	1.75	0.80
4	74	M	L	8	81	1.76	1.22
5	65	M	L	23	84	1.73	0.91
6	37	M	R	80	71	1.75	1.17
7	78	M	L	10	79	1.81	0.96
8	64	M	L	11	75	1.68	1.31
9	72	M	L	15	94	1.80	1.48
10	61	M	L	6	96	1.78	1.13
11	53	F	R	7	78	1.81	1.43
12	67	M	R	38	81	1.75	1.36
13	30	F	L	5	72	1.70	1.15
14	54	F	L	120	91	1.61	1.31
15	66	M	R	36	86	1.90	1.00
Mean	60.0	–	–	26.4	85.3	1.75	1.13
SD	12.94	–	–	32.46	14.62	0.07	0.23
Healthy-control							
1	24	M	–	–	84	1.82	1.32
2	26	M	–	–	75	1.85	1.43
3	22	F	–	–	78	1.57	1.10
4	30	F	–	–	55	1.66	1.51
5	24	M	–	–	66	1.80	1.26
6	21	M	–	–	64	1.78	1.44
7	21	F	–	–	60	1.73	1.34
8	22	F	–	–	82	1.85	1.50
9	22	M	–	–	68	1.65	1.33
10	23	M	–	–	83	1.83	1.27
Mean	23.5	–	–	–	71.4	1.75	1.35
SD	2.76	–	–	–	10.20	0.10	0.13

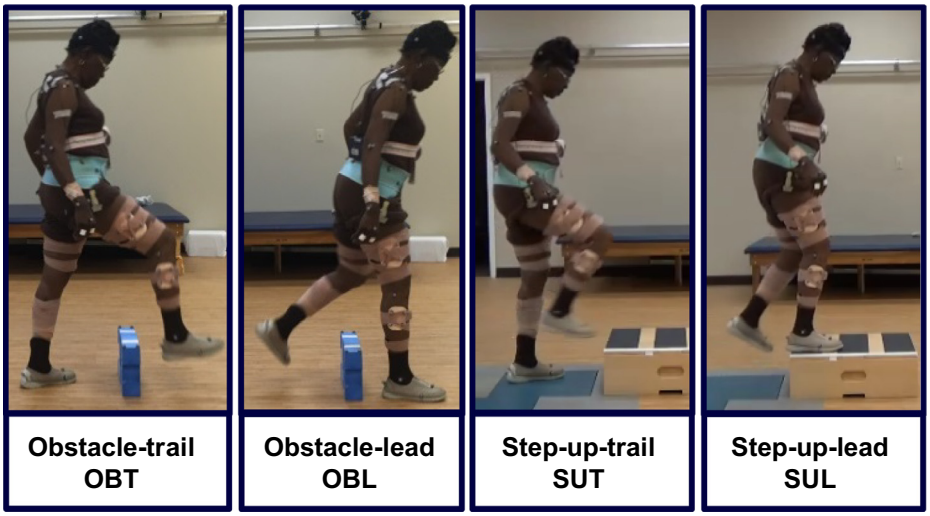

Fig. 2. Walking adaptability tasks were as follows, obstacle-trail (OBT): obstacle negotiation during the trailing leg single-stance; obstacle-lead (OBL): obstacle negotiation during the leading leg single-stance; step-up-trail (SUT): step-up during the trailing leg single-stance; step-up-lead (SUL): step-up during the leading leg single-stance. Each one of the adaptability tasks were repeated for the paretic leg leading as well as the nonparetic leg leading. For example in the OBT, during the paretic single-leg-stance, the nonparetic leg leads to clear the obstacle and vice versa.

velocity vectors of the whole-body CoM. $\overrightarrow{\omega_i}$, m_i and I_i are the angular velocity vector, and mass and moment of inertia of the i-th segment, respectively, and n is the number of segments. Angular-momentum was normalized by the product of subject mass (kg), height (m) and $\sqrt{g \cdot l}$, where g is the gravitational acceleration and l is the subject height. The term $\sqrt{g \cdot l}$ has units of m/s and provides a normalization technique similar to the concept of Froude number (e.g., Vaughan and O'Malley, 2005). Dynamic balance was assessed using the peak-to-peak range of H (H_R), which was calculated as the difference between the minimum and maximum values of H in each plane during the single-leg-stance phase (i.e., paretic leg, nonparetic leg, and average of both legs for the healthy controls). For each task and group, H_R in each plane was averaged across all the trials and participants.

To further understand the regulation of H in the planes where the largest between-group differences were found (suggesting balance deficits), the net external moment and corresponding moment arms were quantified. The net external moment was calculated as the time derivative of the H vector ($\dot{H}$) and averaged during the SLS phase. Foot placements were quantified by the peak external moment arms, which were calculated as the maximum distance between the body CoM to the CoM of the stance foot during the SLS phase and were normalized by body height. For instance, the moment arms in the mediolateral and vertical directions influence the regulation of H in the frontal plane through the generation of net external moment (Fig. 1). The mean $\dot{H}$ and moment arms were calculated across all participants for each task. Also, the duration of SLS for each leg was calculated as a percentage of the gait cycle and was averaged across all participants for each task.

EMG data were high-pass filtered (30 Hz) using a fourth-order Butterworth filter, demeaned, rectified and low-pass filtered (10 Hz) using a fourth-order Butterworth filter. EMG amplitudes in each task were normalized by the mean peak amplitude of the same muscle during the self-selected walking task. Muscle activation in each task was quantified by averaging the normalized EMG amplitudes of each muscle during the single-leg-stance phase.

2.4. Statistical analysis

To test the first hypothesis, H_R in each plane was assessed using separate two factor (limb, task) repeated measures ANOVA and ANCOVA using SPSS (IBM Corp, Armonk, NY, USA). A two-way repeated measures ANOVA was used to compare H_R during the paretic-SLS to the nonparetic-SLS (within-subject), and a mixed-design ANCOVA with covariate (walking speed) was used to compare H_R between the paretic-SLS and healthy control-SLS (between-subject). The task factor in both models consisted of seven levels (self-selected walking, fastest-comfortable walking, backward walking, obstacle-trail, obstacle-lead, step-up-trail, and step-up-lead; Fig. 2). If significant main (limb factor) or interaction (limb∗task) effects were found, pairwise comparisons with Bonferroni adjustments ($\alpha/2$ limb, $\alpha/6$ task, $\alpha = 0.05$) were conducted. If the sphericity was violated in within-subject comparisons, a Greenhouse-Geisser adjustment was applied. The homogeneity of variances was checked using Levene's test for between-subject comparisons. Significant differences in H_R between the paretic- and healthy control-SLS may indicate poor regulation of H, suggesting balance deficits. Significant differences in H_R between the tasks (if consistent in both groups) may be indicative of task requirements. To test the second hypothesis, $\dot{H}$, the corresponding moment arms, and the soleus and medial-gastrocnemius activity were similarly compared between limbs and across tasks. To identify which underlying mechanisms were associated with the regulation of H, Pearson's correlation analyses were performed between H_R and the moment arms and muscle activity that were significantly different between paretic- and healthy control-SLS.

3. Results

The time trajectories of H are shown in each plane (Fig. 3). In the analysis of H_R across tasks, due to similar results between paretic- and nonparetic-SLS, only the paretic-SLS results are presented.

3.1. Sagittal-plane

The analysis of H within each task revealed no significant limb effects (Fig. 4). Across tasks, H_R was higher during the obstacle-trail and step-up-trail tasks than all other tasks in both paretic- and healthy control-SLS (Fig. 5). Due to no significant group effects in H, no further analysis of the underlying biomechanical mechanisms was conducted.

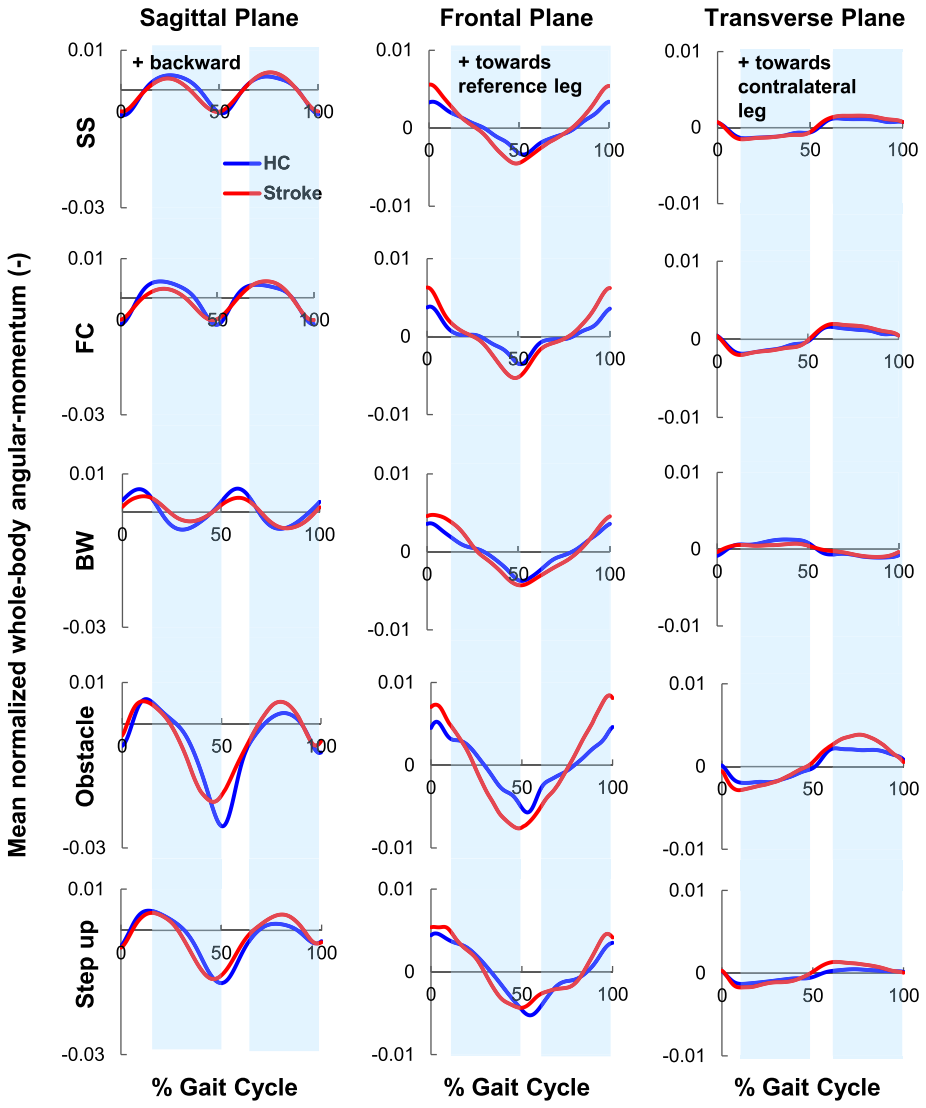

Fig. 3. The mean, normalized trajectories of whole-body angular-momentum in each of the three anatomical planes for all the tasks (SS: self-selected; FC: fastest-comfortable; BW: backward walking; Obstacle: obstacle clearance; Step-up: stepping up a box). Trajectories represent average data across participants post-stroke (red) and healthy controls (blue). The post-stroke data is shown in the paretic leg reference frame (i.e., 0% gait cycle represents paretic leg heel strike). For brevity, only the obstacle and step-up trials leading with the nonparetic leg are shown. Shaded regions represent the healthy control single-leg-stance (SLS) phase of the gait cycle (exact values shown in Fig. 6). Positive directions of angular-momentum are (sagittal: backward; frontal: towards the reference leg; transverse: from the reference leg to the contralateral leg). (For interpretation of the references to color in this figure legend, the reader is referred to the web version of this article.)

3.2. Frontal-plane

The analysis of H within each task revealed significant main (limb) effects ($P = 0.002$) in H_R between the paretic- and healthy control-SLS (Fig. 4). H_R was higher during the paretic- than the healthy control-SLS during self-selected walking ($P = 0.004$), fastest-comfortable walking ($P < 0.001$), obstacle-trail ($P = 0.01$), and obstacle-lead ($P = 0.004$) tasks. Across tasks, H_R during obstacle-trail and obstacle-lead was higher than all other tasks in the paretic-SLS (Fig. 5). However, in healthy controls, H_R during obstacle-trail was only higher than self-selected and fastest-comfortable walking, while H_R during obstacle-lead was similar to self-selected and fastest-comfortable walking tasks (Fig. 5).

Further, in almost all tasks, $\dot{H}$ was higher during the paretic- than nonparetic- and healthy control-SLS. Across tasks, in both paretic- and nonparetic-SLS, $\dot{H}$ during obstacle-trail and obstacle-lead was higher than all other tasks (Fig. 6). However, in healthy controls, $\dot{H}$ during obstacle-trail and obstacle-lead was only higher than the self-selected walking task (Fig. 6). The analysis of external moment arms that influence H in the frontal plane (Fig. 1) revealed that in all tasks both mediolateral and vertical moment arms were higher during the paretic- than healthy control-SLS (Fig. 7). Further, the analysis of muscle activity during the obstacle-trail, obstacle-lead, and step-up-trail tasks revealed lower soleus activation amplitude during the paretic- than healthy control-SLS (Fig. 7). Further, across tasks, healthy adults significantly increased their soleus activation amplitude during the obstacle-trail, obstacle-lead and step-up-trail tasks compared to the self-selected walking task. However, in individuals post-stroke soleus activation during these tasks remained similar to the activation during the self-selected walking task (Fig. 7). No significant group effects were found in the gastrocnemius activation. However, during the obstacle-lead task, the activation amplitude was significantly higher during the paretic- compared to the nonparetic-SLS

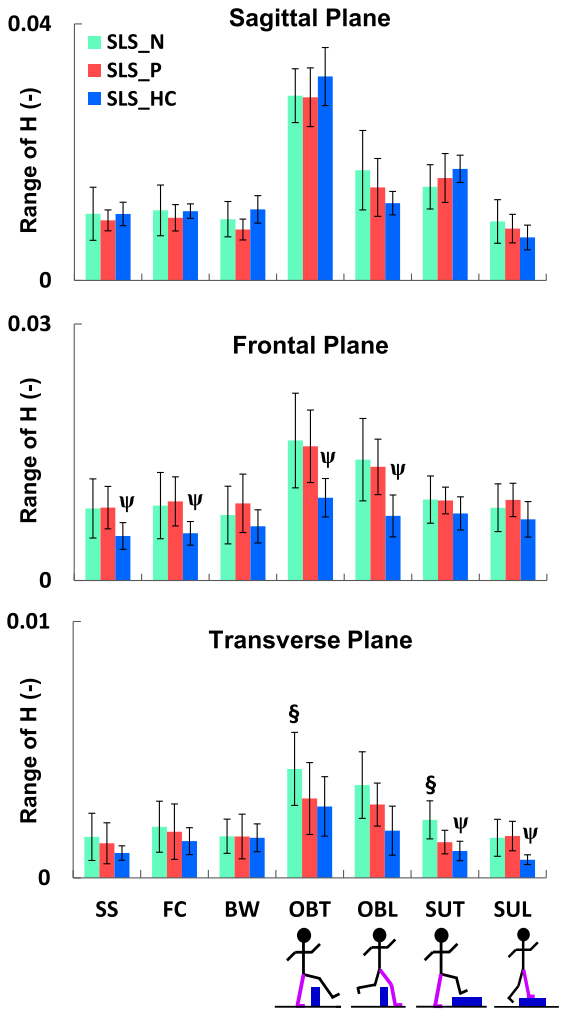

Fig. 4. The mean (SD), normalized range of H (H_R) in each of the three anatomical planes during single-leg-stance (SLS) of the nonparetic leg (green), paretic leg (red), and average of both legs in healthy controls (blue). Tasks included self-selected (SS), fastest-comfortable (FC) and backward (BW) walking, obstacle negotiation during trailing (OBT) and leading (OBL) leg support, and step-up during trailing (SUT) and leading (SUL) leg support. Significant differences ($P < \alpha/2$, $\alpha < 0.05$) are shown between the paretic- and nonparetic-SLS (§) as well as paretic- and healthy control-SLS (ψ). The largest group differences in H_R are in the frontal plane. Note the smaller scale in the transverse plane. (For interpretation of the references to color in this figure legend, the reader is referred to the web version of this article.)

(Fig. 7). Lastly, during all tasks, H_R had moderate to strong correlations with mediolateral and vertical moment arms (Table 2). Also, soleus activation during the obstacle-trail task was inversely correlated with both H_R (r = −0.35, p = 0.08) and $\dot{H}$ (r = −0.45, p = 0.025).

3.3. Transverse-plane

The analysis of H within each task revealed significant limb and task interactions ($P = 0.01$) in H_R between the paretic- and nonparetic-SLS (Fig. 4). H_R was lower during the paretic- than the nonparetic-SLS in the obstacle-trail ($P = 0.001$) and step-up-trail ($P = 0.002$) tasks. In addition, marginal significant main (limb) effects ($P = 0.045$) were found between H_R during the paretic- and healthy control-SLS (Fig. 4). Further, H_R was higher during the paretic- than the healthy control-SLS during the step-up-trail ($P = 0.016$) and step-up-lead ($P = 0.002$) tasks. Across tasks, H_R was higher during the obstacle-trail task than all other tasks in both paretic- and healthy control-SLS (Fig. 5). Due to marginal significant main (group) effects and small H_R values (Fig. 5), no further analyses were performed in this plane.

4. Discussion

Our first hypothesis that across all tasks, significant balance deficits would be evident during the paretic-SLS was primarily supported in the frontal plane (Fig. 4). However, in the sagittal plane, no significant deficits in the regulation of H were found post-stroke (Fig. 4). Further, during the obstacle-trail and step-up-trail tasks, the increases in sagittal-plane H_R relative to the self-selected walking task, observed in both individuals post-stroke and healthy adults (Fig. 5), were likely due to a task requirement for generating a higher forward angular-momentum (Fig. 3) rather than H_R increases due to regulation deficits. In the transverse plane, consistent with prior research (Silverman et al., 2012), we found that during all tasks H_R was nearly an order of magnitude smaller than in the frontal and sagittal planes (Figs. 4 and 5). Thus, during these tasks, the regulation of H in the transverse plane may have smaller contributions to dynamic balance when compared to the frontal and sagittal planes.

In the frontal plane, individuals post-stroke had a higher H_R than healthy adults during the self-selected walking, fastest-comfortable walking, obstacle-trail, and obstacle-lead tasks (Fig. 4). In addition, H_R comparisons across tasks within each group revealed that during the obstacle negotiation task, H_R in healthy adults was similar to other tasks, yet H_R post-stroke was over 70% higher than all other tasks (Fig. 5). These results suggest that increases in the frontal-plane angular-momentum generation post-stroke were less likely due to task requirements and most likely due to deficits in regulation of H. In order to further understand the regulation of H in the frontal plane and identify differences in the underlying mechanisms used in each group, $\dot{H}$, mediolateral and vertical moment arms (i.e., separation between stance foot and body CoM) as well as activation amplitudes of ankle plantarflexor muscles were assessed.

Our second hypothesis that individuals post-stroke use different mechanisms for regulating H than healthy adults was supported. During almost all tasks, $\dot{H}$ was higher during the paretic-SLS than nonparetic- and healthy control-SLS (Fig. 6). In addition, consistent with prior studies (e.g., Olney and Richards (1996), the duration of the paretic-SLS was shorter than nonparetic- and healthy control-SLS (Fig. 6). Hence, during the paretic-SLS, a higher $\dot{H}$ and a shorter SLS duration resulted in a similar H_R as that during the nonparetic-SLS created by a lower $\dot{H}$ and longer SLS duration (Fig. 6). That is, although there were no significant differences in the frontal-plane H_R between the paretic- and nonparetic-SLS (Fig. 4), H was regulated differently between the two limbs. Nott et al. (2014) reported that during steady-state walking, a higher $\dot{H}$ in the frontal plane during the paretic-SLS was associated with poor clinical balance scores (BBS and DGI) and a higher risk of falls. Our results indicate that individuals post-stroke increase their $\dot{H}$ even further during the obstacle negotiation task by over 67% of that during the steady-state walking (Fig. 6). This increase in $\dot{H}$ may place these individuals at an even higher risk of falls. It is important to note that the adults post-stroke in Nott et al. (2014) had likely lower functional level and walking capacity (majority of the participants had a walking speed below 0.8 m/s) than participants in our study. The analysis of H in the current study and Nott et al. suggest that H is sensitive to changes in dynamic balance in a wide range of participants, particularly those with higher walking function, for whom some of the clinical measures can show ceiling effects (Balasubramanian, 2015; Blum and Korner-Bitensky, 2008).

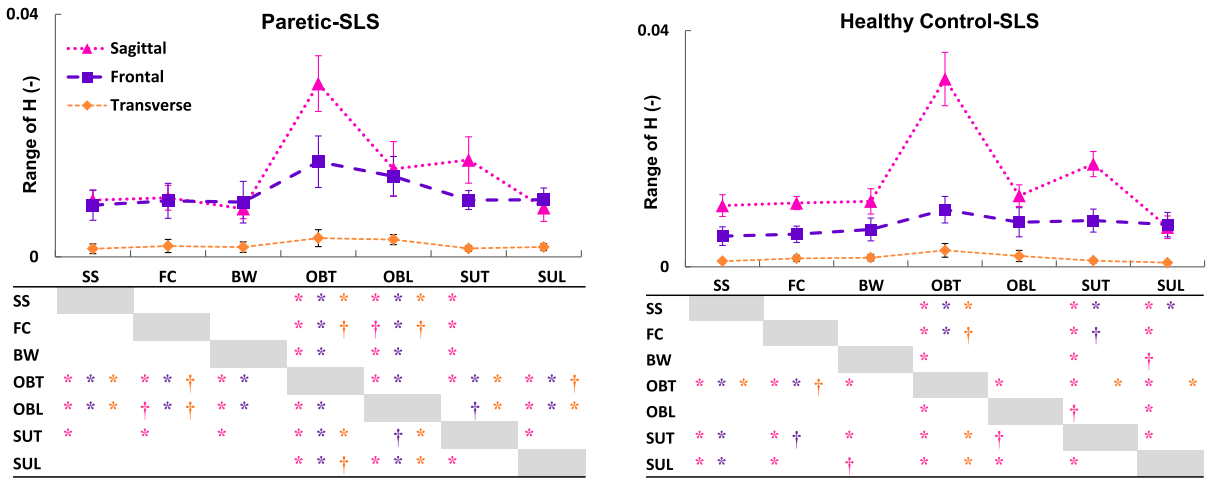

Fig. 5. The mean (SD), normalized range of H (H_R) in the sagittal (▲), frontal (■) and transverse (♦) planes during the paretic and healthy control single-leg-stance (SLS). Significant differences across the tasks are shown in the tables with '*' (for $P < \alpha/6$, $\alpha < 0.01$) and '†' (for $P < \alpha/6$, $0.01 < \alpha < 0.05$). The colors of the significance symbols correspond to the anatomical planes. In the sagittal plane, in both groups H_R during the trailing phase of the obstacle (OBT) and step-up (SUT) tasks was higher than other tasks (task demand). In the frontal plane, only in adults post-stroke H_R during the obstacle negotiation (OBT and OBL) was higher than other tasks (difference in regulation). (For interpretation of the references to colour in this figure legend, the reader is referred to the web version of this article.)

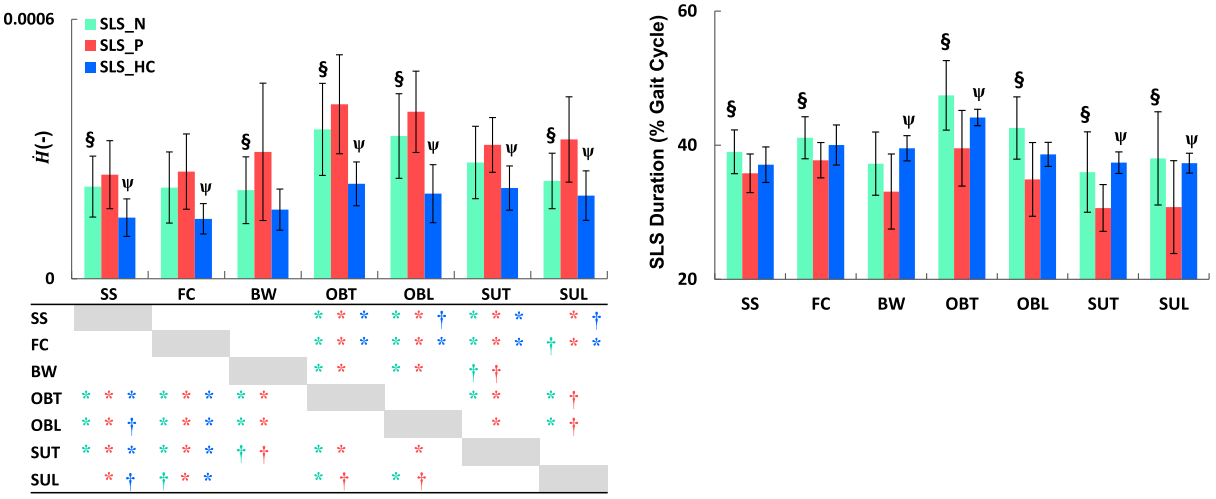

Fig. 6. The mean (SD) rate of change of H ($\dot{H}$) in the frontal plane (left) and single-leg-stance (SLS) duration (right) during the nonparetic (green), paretic (red), and healthy control (blue) SLS. Significant differences ($P < \alpha/2$, $\alpha < 0.05$) are shown between the paretic- and nonparetic-SLS (§) as well as the paretic- and healthy control-SLS (ψ). Significant differences in $\dot{H}$ across tasks are shown in the table with '*' (for $P < \alpha/6$, $\alpha < 0.01$) and '†' (for $P < \alpha/6$, $0.01 < \alpha < 0.05$). The colors of the significance symbols correspond to the limbs. During the paretic-SLS, $\dot{H}$ was higher than the nonparetic- and healthy control-SLS, while paretic-SLS duration was lower than the non-paretic and healthy control-SLS. Adults post-stroke regulated H differently across tasks than healthy controls. (For interpretation of the references to color in this figure legend, the reader is referred to the web version of this article.)

There may be several factors contributing to the higher $\dot{H}$ and the corresponding H_R during the paretic-SLS. Since the rate of change of H is equivalent to the net external moment about the body CoM, a higher $\dot{H}$ indicates a higher net external moment generation. Further, the net external moment in the frontal plane is determined by foot placement (mediolateral and vertical moment arms) as well as mediolateral and vertical ground-reaction-forces (e.g., Silverman et al., 2012). Prior studies have shown that individuals post-stroke generally maintain their body CoM closer to their nonparetic leg (e.g., Bensoussan et al., 2008; Wall and Turnbull, 1986), resulting in a greater distance between body CoM and the paretic leg. Consistent with these findings, our results showed that during almost all tasks, the mediolateral moment arm during the paretic-SLS was significantly wider than during healthy control-SLS (Fig. 7). Further, a higher mediolateral moment arm was associated with a higher H_R (Table 2), which was previously shown to be correlated with poorer BBS and DGI scores (Vistamehr et al., 2016). In addition, during all tasks, the vertical moment arm (i.e., body CoM elevation) was significantly higher during the paretic-SLS than the healthy control-SLS (Fig. 7), which was associated with a higher H_R (Table 2). The elevated CoM position post-stroke may be related to the compensatory mechanisms such as pelvic hiking and hip circumduction during the swing phase (Perry, 1992). Overall, the direction (increase or decrease) of changes in the moment arms across tasks were similar in individuals post-stroke and healthy adults (Fig. 7). However, individuals post-stroke had significantly larger separations between their body CoM and the paretic foot in the mediolateral and vertical directions (Fig. 7).

In addition to foot placement, muscle forces are primary contributors to the regulation of H through the generation of ground-reaction-forces. Specifically, during steady-state walking,

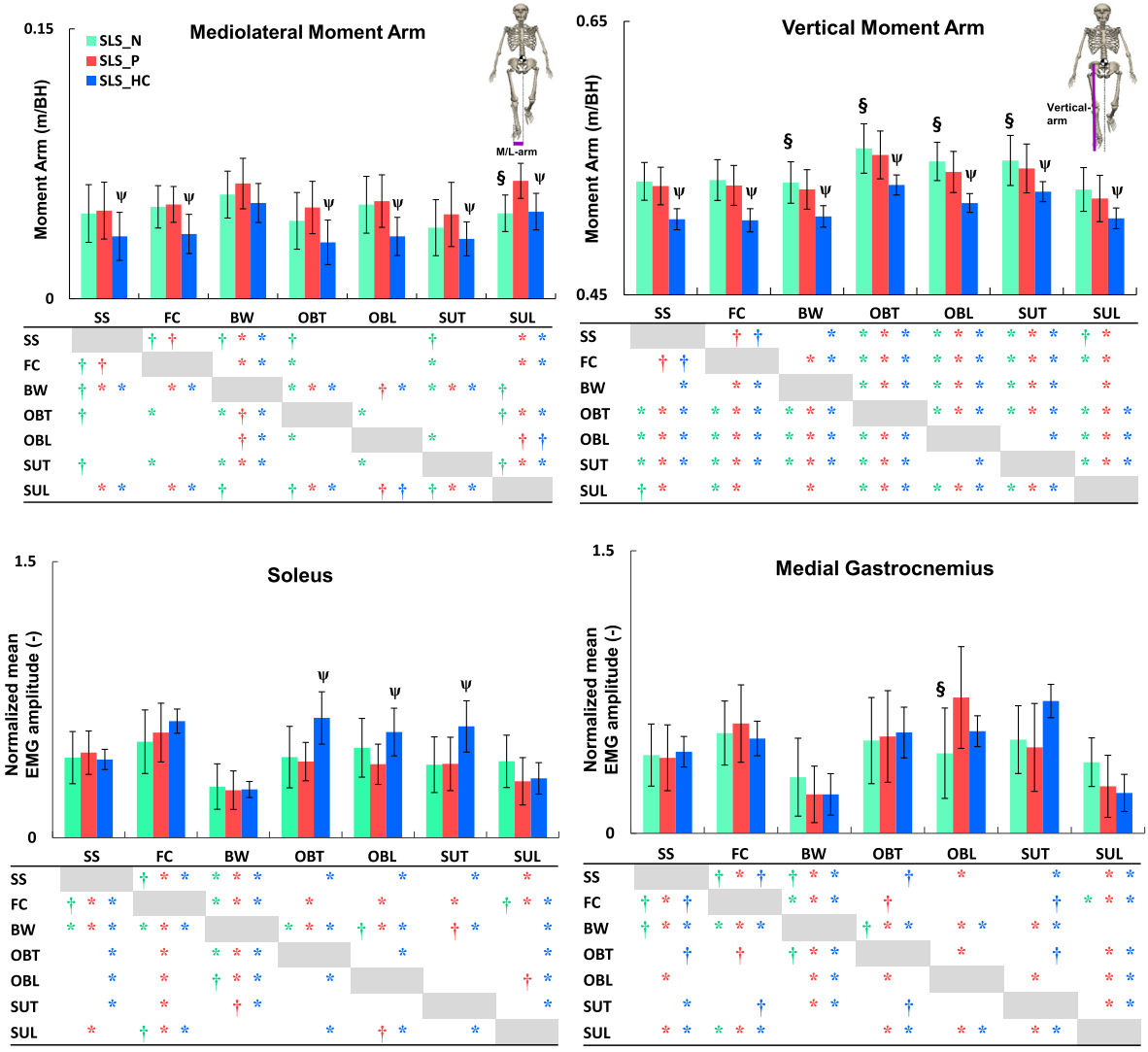

Fig. 7. The mean (SD) mediolateral moment arm (top left); vertical moment arm (top right), soleus (SOL) activation (bottom left); medial gastrocnemius (GAS) activation (bottom right) during the nonparetic (green), paretic (red), and healthy control (blue) single-leg-stance (SLS). Significant differences ($P < \alpha/2$, $\alpha < 0.05$) are shown between the paretic- and nonparetic-SLS (§) as well as the paretic- and healthy control-SLS (ψ). Significant differences across tasks are shown in the tables with '*' (for $P < \alpha/6$, $\alpha < 0.01$) and '†' (for $P < \alpha/6$, $0.01 < \alpha < 0.05$). The colors of the significance symbols correspond to the limbs. Although the direction (increase or decrease) of changes in the moment arms between tasks were similar in both groups, adults post-stroke had significantly larger moment arms than healthy controls. Soleus activation during the obstacle and step-up tasks was significantly higher in healthy controls than post-stroke. (For interpretation of the references to color in this figure legend, the reader is referred to the web version of this article.)

Table 2
Pearson's correlations between H_R and the mediolateral (M/L) and vertical moment arms. Correlations are conducted on combined data from the paretic and healthy control-SLS. Significant correlations ($P < \alpha/2$, $\alpha < 0.05$) are shown with '*'.

Correlations (n = 25)		SS	FC	BW	OBT	OBL	SUT	SUL
H_R and M/L moment arm	r	0.64	0.72	0.66	0.67	0.62	0.60	0.43
	P	0.001*	0.000*	0.001*	0.000*	0.002*	0.003*	0.064
H_R and vertical moment arm	r	0.61	0.53	0.34	0.50	0.75	0.27	0.50
	P	0.002*	0.013*	0.181	0.019*	0.000*	0.370	0.021*

the plantarflexors act to rotate the body towards the contralateral leg while the gluteus medius acts to rotate the body towards the ipsilateral leg (Neptune and McGowan, 2016). Thus, appropriate muscle force generation is necessary to produce the needed external moment to regulate H. Our results showed that during the obstacle-trail, obstacle-lead and step-up-trail tasks soleus activity was significantly lower in the paretic leg than healthy adults (Fig. 7). Further, a lower soleus activation during the obstacle-trail task was associated with a higher H_R ($r = -0.35$, $p = 0.08$) and $\dot{H}$($r = -0.45$, $p = 0.025$). Plantarflexor weakness is a common impairment post-stroke (e.g., Nadeau et al., 1999) and likely responsible for the poor regulation of H during the paretic-SLS.

Future research should consider confirming these findings using muscle strength measures given that activation magnitude is not necessarily an indication of strength. The obstacle-trail task was particularly interesting due to the highest level of H generation combined with the specific task requirements. In this task, H_R during the paretic-SLS increased by 200% (i.e., tripled), relative to the self-selected walking in the sagittal plane and 84% and 130% in the frontal and transverse planes, respectively (Fig. 5). Thus, during the paretic-SLS, obstacle-trail task required regulation of higher levels of H in all the planes over a prolonged SLS period. Given that the ankle plantarflexors are the primary contributors to the regulation of H in both the sagittal (Neptune and McGowan, 2011) and frontal (Neptune and McGowan, 2016) planes during steady-state walking, the regulation of H during the obstacle-trail task may be especially challenging for adults post-stroke. Lastly, Said et al. (2013) have identified a higher incidence of falls in individuals post-stroke who failed obstacle crossing, highlighting the clinical importance of this task.

A potential limitation of this study is that the healthy adults were not age-matched to the individuals post-stroke. Younger adults were chosen to provide reference data from those with unimpaired balance control. Future work will assess the effect of age on the regulation of H in healthy younger and older adults. Another potential limitation is that the study did not include ground-reaction-force and center-of-pressure data. However, the feasibility of collecting such data during several adaptability tasks is limited as it requires sophisticated equipment as well as additional walking trials, which individuals post-stroke may not be able to endure. However, to gain more insight into some of the underlying mechanisms for ground-reaction-force adaptations, we have examined plantarflexor muscle activity, which may be more clinically relevant. Also, in order to calculate the external moment arm in the mediolateral direction, each foot center-of-mass location was used instead of the center-of-pressure. We have verified separately that during single-leg-stance of steady-state walking there is little change in the center-of-pressure location in the mediolateral direction and that the foot center-of-mass location is within 3% of the center-of-pressure data. We believe similar values would be observed during single-leg-stance in the other tasks and any differences would have minimal influence on our results. Another limitation was that this study did not include any clinical data from the participants. Future studies are needed to expand this work and interpret the biomechanical data in the context of participants' clinical characteristics. Lastly, this study focused on analysis of H during the single-leg-stance phase. Future studies may focus on specific adaptability tasks and analyze the regulation of H during all regions of the gait cycle.

5. Conclusions

To our knowledge this study is the first to quantify dynamic balance during walking adaptability tasks. During all the walking tasks, individuals post-stroke had significant deficits regulating whole-body angular-momentum in the frontal plane, suggesting dynamic balance impairments in the mediolateral direction, particularly during the paretic-SLS. The poor regulation of whole-body angular-momentum was associated with a wider paretic foot placement, an elevated center-of-mass, and lower soleus muscle activity. Thus, interventions focused on addressing these post-stroke impairments may help improve overall walking adaptability and community mobility. In addition, incorporating rehabilitation interventions to improve obstacle negotiation and focusing on the trailing leg single-stance phase may be an effective approach for improving dynamic balance and walking adaptability in individuals post-stroke.

Acknowledgements

The authors acknowledge the valuable contributions from Christy Conroy, MSPT and Paul Freeborn, BS in assisting with data collection and preprocessing. The authors also thank Jessica Howarth, DPT, NCS and Brooke Hoisington, MPT for assisting with testing and subject recruitment. This work was supported by Brooks Collaborative Funding and the Brooks-PHHP Research Collaboration, K12 Rehabilitation Research Career Development Program (NIH/NICHD K12 HD055929), and the VA R R&D Service. The contents are solely the responsibility of the authors and do not necessarily represent the official views of the NIH or the VA.

Conflict of interest

There are no conflicts of interest.

References

Allen, J.L., Kautz, S.A., Neptune, R.R., 2014. Forward propulsion asymmetry is indicative of changes in plantarflexor coordination during walking in individuals with post-stroke hemiparesis. Clin. Biomech. (Bristol, Avon) 29, 780–786.
Balasubramanian, C.K., 2015. The community balance and mobility scale alleviates the ceiling effects observed in the currently used gait and balance assessments for the community-dwelling older adults. J. Geriatr. Phys. Ther. 38, 78–89.
Balasubramanian, C.K., Clark, D.J., Fox, E.J., 2014. Walking adaptability after a stroke and its assessment in clinical settings. Stroke Res. Treat. 2014, 591013.
Bensoussan, L., Viton, J.M., Barotsis, N., Delarque, A., 2008. Evaluation of patients with gait abnormalities in physical and rehabilitation medicine settings. J. Rehabil. Med. 40, 497–507.
Blum, L., Korner-Bitensky, N., 2008. Usefulness of the Berg Balance Scale in stroke rehabilitation: a systematic review. Phys. Ther 88, 559–566.
Forster, A., Young, J., 1995. Incidence and consequences of falls due to stroke: a systematic inquiry. BMJ 311, 83–86.
Hall, A.L., Bowden, M.G., Kautz, S.A., Neptune, R.R., 2012. Biomechanical variables related to walking performance 6-months following post-stroke rehabilitation. Clin. Biomech. (Bristol, Avon) 27, 1017–1022.
Herr, H., Popovic, M., 2008. Angular momentum in human walking. J. Exp. Biol. 211, 467–481.
Hill, K., Ellis, P., Bernhardt, J., Maggs, P., Hull, S., 1997. Balance and mobility outcomes for stroke patients: a comprehensive audit. Aust. J. Physiother. 43, 173–180.
Nadeau, S., Gravel, D., Arsenault, A.B., Bourbonnais, D., 1999. Plantarflexor weakness as a limiting factor of gait speed in stroke subjects and the compensating role of hip flexors. Clin. Biomech. (Bristol, Avon) 14, 125–135.
Neptune, R.R., McGowan, C.P., 2011. Muscle contributions to whole-body sagittal plane angular momentum during walking. J. Biomech. 44, 6–12.
Neptune, R.R., McGowan, C.P., 2016. Muscle contributions to frontal plane angular momentum during walking. J. Biomech. 49, 2975–2981.
Nott, C.R., Neptune, R.R., Kautz, S.A., 2014. Relationships between frontal-plane angular momentum and clinical balance measures during post-stroke hemiparetic walking. Gait Posture 39, 129–134.
Olney, S.J., Richards, C., 1996. Hemiparetic gait following stroke. Part I: Characteristics. Gait Posture 4, 136–148.
Perry, J., 1992. Gait analysis: normal and pathological function.
Pickle, N.T., Wilken, J.M., Aldridge, J.M., Neptune, R.R., Silverman, A.K., 2014. Whole-body angular momentum during stair walking using passive and powered lower-limb prostheses. J. Biomech. 47, 3380–3389.
Pijnappels, M., Bobbert, M.F., van Dieen, J.H., 2005a. How early reactions in the support limb contribute to balance recovery after tripping. J. Biomech. 38, 627–634.
Pijnappels, M., Bobbert, M.F., van Dieen, J.H., 2005b. Push-off reactions in recovery after tripping discriminate young subjects, older non-fallers and older fallers. Gait Posture 21, 388–394.
Robert, T., Bennett, B.C., Russell, S.D., Zirker, C.A., Abel, M.F., 2009. Angular momentum synergies during walking. Exp Brain Res 197, 185–197.
Said, C.M., Galea, M.P., Lythgo, N., 2013. People with stroke who fail an obstacle crossing task have a higher incidence of falls and utilize different gait patterns compared with people who pass the task. Phys Ther 93, 334–344.
Sheehan, R.C., Beltran, E.J., Dingwell, J.B., Wilken, J.M., 2015. Mediolateral Angular Momentum Changes in Persons With Amputation During Perturbed Walking. Gait Posture 41, 795–800.
Silverman, A.K., Neptune, R.R., 2011. Differences in whole-body angular momentum between below-knee amputees and non-amputees across walking speeds. J. Biomech. 44, 379–385.
Silverman, A.K., Neptune, R.R., Sinitski, E.H., Wilken, J.M., 2014. Whole-body angular momentum during stair ascent and descent. Gait Posture 39, 1109–1114.
Silverman, A.K., Wilken, J.M., Sinitski, E.H., Neptune, R.R., 2012. Whole-body angular momentum in incline and decline walking. J. Biomech. 45, 965–971.

Vaughan, C.L., O'Malley, M.J., 2005. Froude and the contribution of naval architecture to our understanding of bipedal locomotion. Gait Posture 21, 350–362.
Vistamehr, A., Kautz, S.A., Bowden, M.G., Neptune, R.R., 2016. Correlations between measures of dynamic balance in individuals with post-stroke hemiparesis. J. Biomech. 49, 396–400.
Wall, J.C., Turnbull, G.I., 1986. Gait asymmetries in residual hemiplegia. Arch. Phys. Med. Rehabil. 67, 550–553.
Yeates, K.H., Segal, A.D., Neptune, R.R., Klute, G.K., 2016. Balance and recovery on coronally-uneven and unpredictable terrain. J. Biomech. 49, 2734–2740.